Original Research Article

GREENHOUSE GASES SCIENCE AND TECHNOLOGY

Experimental investigation on CO_2 desorption kinetics from MDEA + PZ and comparison with MDEA/MDEA + DEA aqueous solutions with thermo-gravimetric analysis method

Shunji Kang, Key Laboratory for Green Chemical Process, Ministry of Education, School of Chemical Engineering and Pharmacy, Wuhan Institute of Technology, Wuhan, China and The College of Post and Telecommunication of WIT, Wuhan, China
Zhi Shen, Xizhou Shen and Liuya Fang, Key Laboratory for Green Chemical Process, Ministry of Education, School of Chemical Engineering and Pharmacy, Wuhan Institute of Technology, Wuhan, China
Li Xiang, The College of Post and Telecommunication of WIT, Wuhan, China
Wenze Yang, Central Southern China Electric Power Design Institute, Wuhan, China

Abstract: The carbon dioxide discharged from fossil fuels combustion products is considered as a major contributor to global warming. The current investigation aimed at CO_2 desorption kinetics in 3.25 mol L^{-1} methyldiethanolamine (MDEA)–0.1 mol L^{-1} piperazine (PZ) rich amine aqueous solution with thermo-gravimetric analysis (TGA) method under different heating rates of 2.5, 5, 10, and 20 °C min^{-1}. The kinetics parameters were determined by comparison of 40 mechanism functions with thermal analysis kinetic method. The average activation energy E was 59.16 kJ mol^{-1}, preexponential factor A was 5.54×10^8, and the most probable mechanism function was $G(\alpha) = [-\ln(1-\alpha)]^{3/2}$. In addition, the kinetic parameters of CO_2 desorption process from three rich amine aqueous solutions (MDEA, MDEA + diethanolamine(DEA), MDEA + PZ) were compared and the influence of kinetic parameters was further discussed. The desorption rate models of three rich amine aqueous solutions were established and desorption rates were well predicted. The order of desorption rate inferred from desorption rate model was MDEA > MDEA + DEA > MDEA + PZ. The results indicated that TGA combined with thermal analysis kinetics was an effective and quick method with high accuracy, easy operation, and good repeatability for screening absorbents preliminarily in laboratory. © 2021 Society of Chemical Industry and John Wiley & Sons, Ltd.

Keywords: desorption kinetics; MDEA + PZ; thermal analysis kinetics; thermo-gravimetric method

Correspondence to: Zhi Shen and Xizhou Shen, Key Laboratory for Green Chemical Process, Ministry of Education, School of Chemical Engineering and Pharmacy, Wuhan Institute of Technology, Wuhan, China.
E-mail: shenzhi20121111@163.com
Received June 4, 2020; revised July 9, 2021; accepted July 16, 2021
Published online at Wiley Online Library (wileyonlinelibrary.com). DOI: 10.1002/ghg.2107

Introduction

Global warming is a serious challenge to human environment, and the Paris Agreement signed by 178 countries took effect on November 4, 2016. It starts a new stage for global climate disposal and reducing CO_2 emission. Therefore, postcombustion CO_2 capture has become an issue attracting widespread attention to find out a highly efficient CO_2 capture technique towards mitigation of greenhouse gas.[1,2] It is well known that CO_2 can be removed by means of various approaches such as physical absorption, chemical absorption, cryogenic distillation, membrane separation, and so on. Especially, chemical absorption is generally recognized as the most effective method due to the advantages of outstanding absorption efficiency and recycling capacity.[3,4] The chemical absorbents, such as potassium carbonate, sodium carbonate, ammonia, and alkanolamine, were applied for CO_2 absorption.[5–7] MDEA is widely regarded as an appropriate absorbent for postcombustion CO_2 capture in industry due to its advantages of less degradation, high reliability, low energy consumption, and greater suitability. The famous chemical enterprise from Germany, Badische Anilin-und-Soda-Fabrik (BASF) has developed the first CO_2 capture facility with MDEA in ammonia plant. Noticeably, the absorption efficiency of blended amine aqueous solutions is superior to single solvent. Researchers have always focused on adding activators (e.g., monoethanolamine [MEA], DEA, triethylenetetramine [TETA], 2-amino-2-methyl-1-propanol [AMP], and PZ) to improve MDEA absorption effect.[8–14]

PZ is widely accepted as an efficient activator to MDEA. Xu studied the effect on CO_2 loading in MDEA + PZ aqueous solution and reported that PZ was beneficial for CO_2 loading in MDEA aqueous solution.[15] Ali used PZ as activator at concentration ranging from 0.01–0.1M in 2M MDEA. The result indicated that addition of PZ could increase the CO_2 solubility at low CO_2 partial pressure compared to pure MDEA.[16] Note that 4 M MDEA + 0.05 M PZ blend aqueous solution was used to remove CO_2 in a semi-batch stirred cell with continuous operation. The result showed that CO_2 absorption rate was strongly influenced by PZ and it conformed with "activation" mechanism.[17] Nevertheless, the energy consumption of desorption process undoubtedly accounts for the major cost of the whole CO_2 capture process in industry. Reduction of the regeneration energy has great commercial prospect. Consequently, an efficient absorbent should not only present good absorption performance but also need high desorption rate and lower regeneration energy.

However, the operation condition and desorption device would impact the desorption rate and there are various kinds of desorption devices, such as stirred tank reactor, stopped-flow technique, stirred cell, wetted wall column, microchannel reactor and hollow fiber membrane contactor and so on. Xu studied the desorption kinetics of PZ in MDEA and established desorption model in a packed column. The desorption rate from PZ activated MDEA solution were about $1–4\times10^{-4}$ kmol·m^{-3-1}.[18] Renaud studied kinetics of CO_2 desorption from MDEA solutions (25 and 50 wt%) in a $(6.20 \pm 0.02) \times 10^{-2}$ internal diameter thermostated glass reactor. The desorption rate were about $3.39\times10^{-6}\sim1.1\times10^{-4}$ mol·m—^{2}·s^{-1}.[19] Aqil researched the CO_2 absorption and desorption in aqueous alkanolamine solutions in a novel hemispherical contactor. The result showed that MDEA desorbed much faster compared to DEA and MEA.[20] A novel direct steam stripping process had been studied for simulating CO_2 desorption in three typical solvents, MEA, PZ, and AMP. For the same rich loading CO_2 amine, the minimum regeneration energy penalty for AMP, MEA, and PZ were 3.064, 3.034, and 2.749 GJ/tCO_2.[21] Zhang studied absorption–desorption performance for blends of MEA, MDEA ,and PZ with magnetic stirrer in oil bath and the results showed that MDA–MDEA–PZ had lower absorption heat than single amine solution. The energy consumption decreased and CO_2 desorption rate increased as the ratio of MDEA-PZ increased.[22] Aghel studied CO_2 desorption from aqueous solutions of MEA and DEA in a microchannel reactor. The results also showed that the liquid phase mass transfer coefficient $k_L\alpha_v$ for the two solvents of MEA and DEA was 1.91 and 3.48 s^{-1}, respectively.[23] Barzagli investigated CO_2 absorption and desorption in DEA and MDEA solutions with ^{13}C NMR spectroscopy. The change of CO_2 content, formation time, and temperature of reaction product could be monitored accurately with this method. The average amine regeneration efficiency were 69.6% (DEA) and 78.23% (MDEA).[24] Listiyana investigated CO_2 desorption from activated DEA in hollow fiber membrane contactor by adding arginine, PZ, and K_2CO_3. The experimental result showed that increasing operation temperature

could enhance CO_2 desorption flux and regeneration efficiency.[25] Liu has investigated the enhancement of CO_2 desorption from MDEA rich amine aqueous solution in ultrasonic microreactor. The results indicated that regeneration energy consumption and solvent loss could be efficiently reduced, and ultrasound method could intensify the CO_2 desorption at low temperature.[26] Among the researches, stripping apparatus and thermal regeneration are mainly used for CO_2 desorption in experiment. Stripping in pilot plant has a positive effect in improving mass transfer and reducing the equilibrium pressure of CO_2 in gas side, which is conducive to desorption. The thermal regeneration method is generally used in laboratory. Virtually the desorption performance is influenced by different factors such as concentration of solvent, ratio of activator, chemical and physical characteristics of absorbent, temperature, pressure, device structure, analyzing approach, monitoring method, and control instrument. In this paper, the CO_2 desorption kinetics in MDEA + PZ aqueous solution at different heating rates has been investigated with TGA method. The desorption kinetic parameters (mechanism function $G(\alpha)$, activation energy E, and prefactor A) of MDEA + PZ system were determined by thermal analysis kinetics. Moreover, the study on CO_2 desorption kinetics in MDEA and MDEA + DEA rich amine aqueous solutions has been well executed with TGA in our previous work. The desorption kinetic models of three rich amine aqueous solutions (MDEA, MDEA + DEA, and MDEA + PZ) could be established and discussed further in order to evaluate desorption performance.

Experiment

The analytical grade MDEA (98wt%) and PZ (99%) were both supplied from Shanghai Aladdin biochemical technology Co. Ltd.(China). The thermogravimetric analyzer (PerkinElmer TGA 8000) was used to carry out the thermo-gravimetric analysis experiment. The experiment in this work is the same as previous research.[27]

Rich amine aqueous solution preparation

The concentration of MDEA aqueous solution 3.25mol/L is consistent with concentration of absorbent provided by Sinopec Wuhan corporation 30–40 wt%. The concentration of PZ was about 1% in amine aqueous solution which was converted as 3.25 mol L^{-1} MDEA–0.1 mol L^{-1} PZ. The rich amine aqueous solution 3.25 mol L^{-1} MDEA–0.1 mol L^{-1} PZ was prepared to simulate absorbents in industry. Then CO_2 was fed into a packed tower for 6 hr continuously to prepare the rich amine aqueous solution with high CO_2-loadings in part (1) of Fig. 1. While the deviations of three consecutive samples were less than 1%, it could almost determine that the amine aqueous solutions were saturated with CO_2 and the absorption was nearly in equilibrium. Then the rich amine aqueous solutions with high CO_2-loadings were prepared.[28]

Acid hydrolysis analysis

The solubility of CO_2 in rich amine solution was measured by acid hydrolysis apparatus in Fig. 1, and the content of CO_2 could be calculated.[28] A syringe was used to take samples from the bottom of tower, and sealed the needle with a rubber plug in order to avoid flash evaporation. Then the sample was immediately injected into the acid hydrolysis analysis system.

The amine aqueous solution reacts with CO_2 and form carbamate or bicarbonate. The excess of dilute sulfuric acid is added into rich amine aqueous solution, and the CO_2 will be all released by strong acid. The operations are as follows:

1. First check the air tightness of the analysis system.
2. Lift the reagent flask 1 to keep the liquid level of reagent flask 1 and acid burette equal and then get the reading data V_1.
3. Take 0.5 mL rich amine aqueous solution in syringe and inject into conical flask.
4. Take 5 mL dilute sulfuric acid into a conical flask and shake in order to keep dilute sulfuric acid and rich amine aqueous solution in contact with each other. The CO_2 in the rich amine aqueous solution was desorbed out.
5. Lift the reagent flask 1 again to keep the liquid level of reagent flask 1 and acid burette equal and then get the reading data V_2.
6. The difference between the two readings subtracted the volume of dilute sulfuric acid 5 mL, and then the volume of CO_2 released from rich amine aqueous solution is obtained by $V_{CO_2} = V_2 - V_1 - 5$.
7. According to the gas state equation, the amount of substance desorbed CO_2 is calculated by Eqn (1). The data is the amount of CO_2 absorbed by the

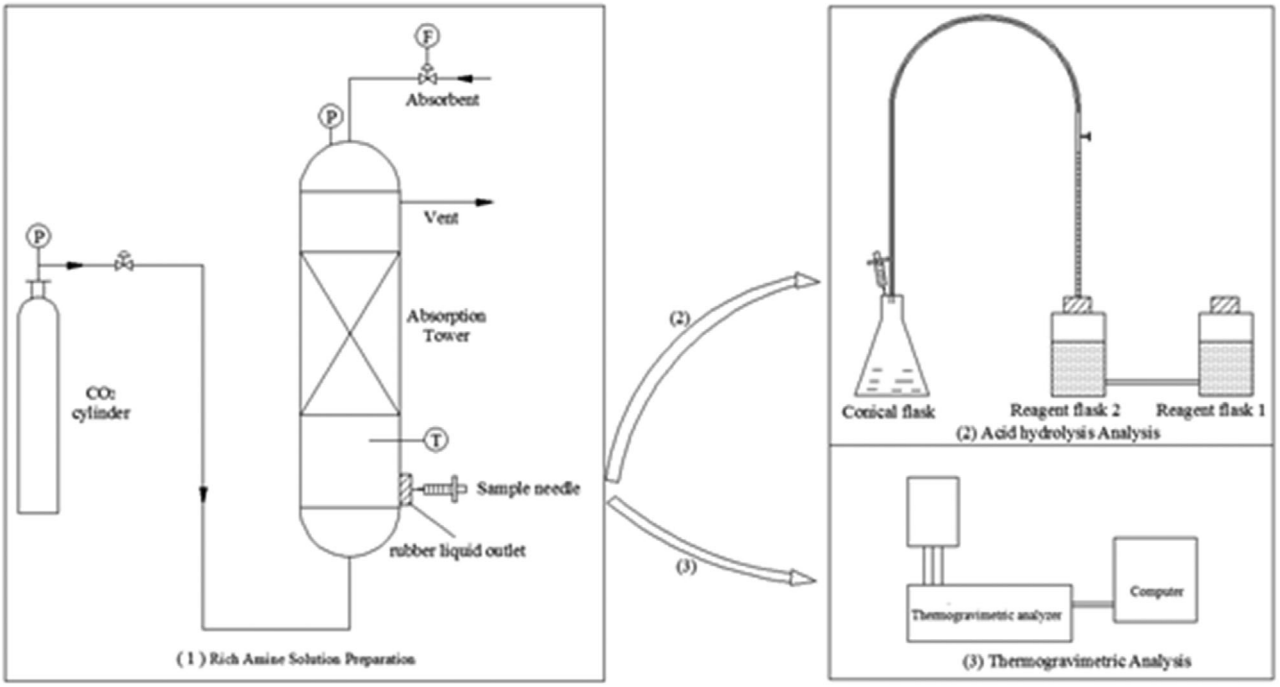

Figure 1. Experiment diagram.

amine aqueous solution and the solubility of CO_2 in the amine aqueous solution can be calculated by Eqn (2).

$$n_{CO_2} = \frac{p_{CO_2} V_{CO_2}}{RT} \tag{1}$$

$$a_{CO_2} = \frac{c_{CO_2}}{c_{MDEA}} \tag{2}$$

where n_{CO_2} is molar weight in rich amine aqueous solution (mol); a_{CO_2} is solubility of CO_2 in amine aqueous solution (mol CO_2 /mol MDEA); c_{CO_2} is the molarity concentration of CO_2 in amine aqueous solution (mol L^{-1}); c_{MDEA} is the concentration of CO_2 in amine aqueous solution (mol L^{-1}).

Thermo–gravimetric analysis

Samples were collected in thoroughly rinsed glass bottles which were sealed tightly to prevent contamination. Take 25–35 mg sample into crucible and put the crucible in thermo-gravimetric analyzer with conditions of heating rates β (2.5, 5, 10, and 20 °C min^{-1}) in the atmosphere of 40 mL min^{-1} N_2 flow. The TG and DTG curves of CO_2 evaporation in rich amine aqueous solutions were obtained. The thermo-gravimetric analysis experiment conditions of heating rate and atmosphere were as same as the previous work to avoid deviation caused by different operating conditions.

Kinetic parameters calculation

The kinetic parameters and model could be established through the research of thermal analysis kinetics of MDEA + PZ rich amine aqueous solution with isoconversional method Flynn–Wall–Ozawa (FWO) and model fitting method Coats–Redfern (CR) .[29–31]

FWO method

The activation energy E is calculated with TG data by FWO method, which is shown in Eqn (3).[29,30]

$$\lg \beta = \lg\left(\frac{AE}{RG(\alpha)}\right) - 2.315 - 0.4567\frac{E}{RT} \tag{3}$$

where α is conversion rate (%); β is heating rate (°C min^{-1}); $G(\alpha)$ is integral mechanism function; A is preexponential factor; E is activation energy.

Equation (3) can be transformed to Eqn (4) as following,

$$\lg \beta = -0.4567\frac{E}{RT} + C \tag{4}$$

Table 1. Mechanism functions.

No.	Integral mechanism function, $G(\alpha)$	Differential mechanism Function, $f(\alpha)$	No.	Integral mechanism function, $G(\alpha)$	Differential mechanism function, $f(\alpha)$
1	α^2	$1/2\alpha^{-1}$	22	$\alpha^{1/4}$	$4\alpha^{3/4}$
2	$\alpha+(1-\alpha)\ln(1-\alpha)$	$[-\ln(1-\alpha)]^{-1}$	23	$\alpha^{1/3}$	$3\alpha^{2/3}$
3	$[1-(1-\alpha)^{1/2}]^{1/2}$	$4(1-\alpha)^{1/2}[1-(1-\alpha)^{1/2})]^{1/2}$	24	$\alpha^{1/2}$	$2\alpha^{1/2}$
4	$[1-(1-\alpha)^{1/2}]^2$	$(1-\alpha)^{1/2}[1-(1-\alpha)^{1/2}]^{-1}$	25	α	1
5	$[1-(1-\alpha)^{1/3}]^{1/2}$	$6(1-\alpha)^{2/3}[1-(1-\alpha)^{1/3}]^{1/2}$	26	$\alpha^{3/2}$	$2/3\alpha^{-1/2}$
6	$[1-(1-\alpha)^{1/3}]^2$	$3/2(1-\alpha)^{2/3}[1-(1-\alpha)^{1/3}]^{-1}$	27	α^2	$1/2\alpha^{-1}$
7	$1-2/3\alpha-(1-\alpha)^{2/3}$	$3/2[(1-\alpha)^{-1/3}-1]^{-1}$	28	$1-(1-\alpha)^{1/4}$	$4(1-\alpha)^{3/4}$
8	$[(1+\alpha)^{1/3}-1]^2$	$3/2(1+\alpha)^{2/3}[(1+\alpha)^{1/3}-1]^{-1}$	29	$1-(1-\alpha)^{1/3}$	$3(1-\alpha)^{2/3}$
9	$[(1-\alpha)^{-1/3}-1]^2$	$3/2(1-\alpha)^{4/3}[(1-\alpha)^{-1/3}-1]^{-1}$	30	$3[1-(1-\alpha)^{1/3}]$	$(1-\alpha)^{2/3}$
10	$[-\ln(1-\alpha)]^{1/4}$	$4(1-\alpha)[-\ln(1-\alpha)]^{3/4}$	31	$1-(1-\alpha)^{1/2}$	$2(1-\alpha)^{1/2}$
11	$[-\ln(1-\alpha)]^{1/3}$	$3(1-\alpha)[-\ln(1-\alpha)]^{2/3}$	32	$2[1-(1-\alpha)^{1/2}]$	$(1-\alpha)^{1/2}$
12	$[-\ln(1-\alpha)]^{2/5}$	$5/2(1-\alpha)[-\ln(1-\alpha)]^{3/5}$	33	$1-(1-\alpha)^2$	$1/2(1-\alpha)^{-1}$
13	$[-\ln(1-\alpha)]^{1/2}$	$2(1-\alpha)[-\ln(1-\alpha)]^{1/2}$	34	$1-(1-\alpha)^3$	$1/3(1-\alpha)^{-2}$
14	$[-\ln(1-\alpha)]^{2/3}$	$3/2(1-\alpha)[-\ln(1-\alpha)]^{1/3}$	35	$1-(1-\alpha)^4$	$1/4(1-\alpha)^{-3}$
15	$[-\ln(1-\alpha)]^{3/4}$	$4/3(1-\alpha)[-\ln(1-\alpha)]^{1/4}$	36	$(1-\alpha)^{-1}$	$(1-\alpha)^2$
16	$-\ln(1-\alpha)$	$1-\alpha$	37	$(1-\alpha)^{-1}-1$	$(1-\alpha)^2$
17	$[-\ln(1-\alpha)]^{3/2}$	$2/3(1-\alpha)(-\ln(1-\alpha))^{-1/2}$	38	$(1-\alpha)^{-1/2}$	$2(1-\alpha)/^{3/2}$
18	$[-\ln(1-\alpha)]^2$	$1/2(1-\alpha)(-\ln(1-\alpha))^{-1}$	39	$\ln\alpha$	α
19	$[-\ln(1-\alpha)]^3$	$1/3(1-\alpha)[-\ln(1-\alpha)]^{-2}$	40	$\ln\alpha^2$	$1/2\alpha$
20	$[-\ln(1-\alpha)]^4$	$1/4(1-\alpha)[-\ln(1-\alpha)]^{-3}$	41	$(1-\alpha)^{-2}$	$1/2(1-\alpha)^3$
21	$\ln[\alpha/(1-\alpha]$	$\alpha(1-\alpha)$			

Equation (4) shows a linear relationship between $\lg\beta-$ and 1/T. The average activation energy E can be calculated according with the slope.

CR method

The kinetic parameters (activation energy E, preexponential factor A and the most probable integral mechanism function) of CO_2 desorbed from MDEA + PZ rich amine aqueous solution at four heating rates (2.5, 5, 10, and 20 °C min^{-1}) can be calculated with 40 mechanism functions $G(a)$ by means of CR method,[27,29] and the results were shown in Table 1.

$$\ln[G(\alpha)/T^2] = \ln\left(\frac{AR}{\beta E}\right) - \frac{E}{RT} \qquad (5)$$

The E and A could be determined by the slope and intercept respectively with liner fitting of $\ln[G(\alpha)/T^2]$ and $1/T$ with CR method in Eqn. (5).

Table 2. Mass fractions of MDEA + PZ rich amine solution.

Solution	MDEA	PZ	H_2O	CO_2
Mass fractions, wt%	34.43	0.77	53.71	11.09

Results and discussion

Thermo-gravimetric analysis of MDEA + PZ rich amine aqueous solution

The mass fraction of MDEA + PZ (3.25 mol L–0.1 mol L) rich amine aqueous solution was measured at condition of 101.3kPa and 298.15 K, and the content of other components could be calculated, which were listed in Table 2. It could be found that mass fraction sum of H_2O and CO_2 was 64.8 wt% theoretically.

The TG curves of MDEA + PZ aqueous solution measured at different heating rates of 2.5, 5, 10, and 20 °C min^{-1} were shown in Fig. 2. The weight decreased quickly as the temperature increasing about

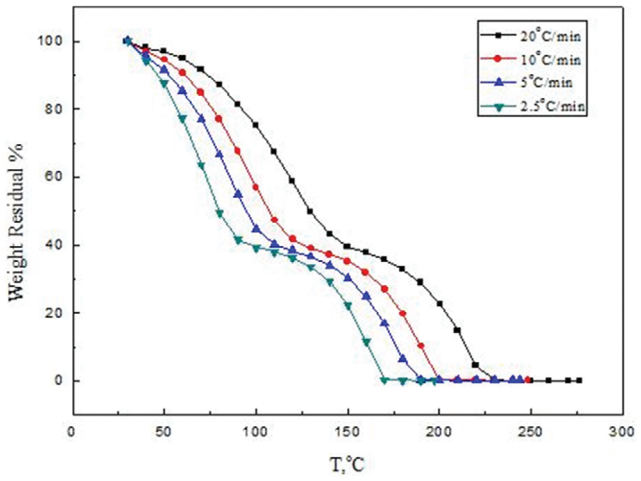

Figure 2. TG curves of MDEA + PZ amine solution at different heating rates.

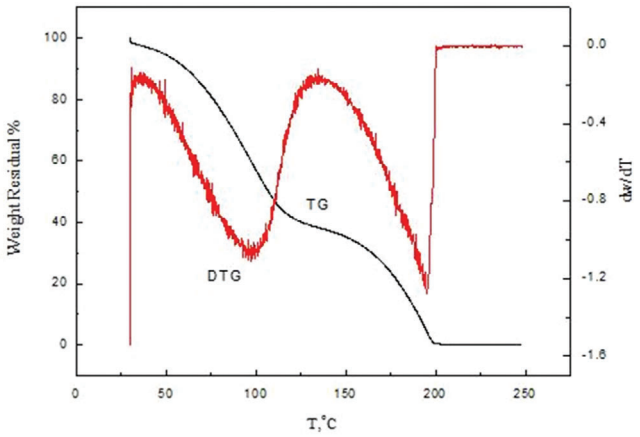

Figure 3. TG-DTG curves of MDEA – PZ amine solution at 10 °C/min

60% at range of 85–135 °C, then the weight decreased slowly for a while, and at last plummet to zero at 100–240 °C. The trends of TG curves of MDEA + PZ aqueous solution were almost the same with that of MDEA and MDEA + DEA rich amine aqueous solutions in previous work.[27] It was inferred that the evaporation process of MDEA + PZ could also be divided into two stages as well as MDEA and MDEA + DEA aqueous solutions. The weight of amine aqueous solution sharply cut down nearly 60–65% at initial stage, and then continually decreased about 35–40% with temperature increasing at the second stage. In addition, the TG curve was on the far left at 2.5 °C min^{-1} and on the far right at 20 °C min^{-1}. The TG curves moved to the right with the heating rate increasing. This phenomenon was caused of heating transfer hysteresis, and the delay was more serious and the temperature range was wider as the heating rate increasing in TG experiment.

Since the trends of TG curves at four heating rates were nearly the same, the DTG curve of heating rate 10 °C min^{-1} was selected as a representation. The TG–DTG curves measured at heating rate of 10 °C min^{-1} were shown in Fig. 3. It was observed that there were two peaks on the DTG curve, which corresponded to two inflection points on TG curve. It further manifested that desorption process of MDEA + PZ rich amine aqueous solution could be divided into two stages.

The weight losses of MDEA + PZ aqueous solution at four heating rates (2.5, 5, 10, 20 °C min^{-1}) in first stage were 65.9, 65.7, 64.6, and 63.3% respectively which were presented in Fig. 4. The average value of weight loss was 64.88%, which was extremely close to the theoretical mass fraction of CO_2 and H_2O 64.8% in Table 2. It can be inferred that CO_2 and H_2O were released from MDEA + PZ rich amine aqueous solution in first stage. Meanwhile, the value of weight loss at second stage was 35.12%, which was almost equal to theoretical mass fraction sum of MDEA and PZ 35.2% in Table 2. It could be indicated that MDEA and PZ with higher boiling points evaporated gradually in second stage. The desorption process of MDEA + PZ rich amine aqueous solution was highly consistent with MDEA and MDEA + DEA system in previous work. It manifested that TGA method was an effective way to research CO_2 desorption from rich amine aqueous solution.

Kinetic parameters for rich amine aqueous solution evaporation

The values of activation energy E at different conversion rates for MDEA + PZ rich amine aqueous solution calculated with FWO method by Eqn (4) and the results were presented in Fig. 5. Activation energy E decreased from 75.67 to 51.75 kJ mol^{-1} with conversion rate increasing from 0.01 to 0.6 and the average value was 54.76 kJ mol^{-1}.

On the other hand, the E and R data of 40 mechanism functions calculated with Eqn (5) were presented in Table 3. Mechanism function with activity energy E value which was highly approximated to value of FWO method and high correlation coefficient R simultaneously would be chosen as the most probable mechanism function for CO_2 desorption kinetics equation. It could be seen in Table 3 that the activation

Table 3. The activation energy E and relative error for MDEA + PZ rich amine solutions with CR method.

	2.5 °C min^{-1}		5 °C min^{-1}		10 °C min^{-1}		20 °C min^{-1}		Ave	
No.	E, kJ mol^{-1}	R^2	E, kJ mol^{-1}	R^2	E, kJ mol^{-1}	R^2	E, kJ/mol	R^2	E	R
1	80.53	0.92386	67.99	0.95248	64.99	0.95271	59.57	0.96435	68.27	0.9738
2	85.09	0.93437	71.82	0.96097	68.68	0.96137	62.97	0.97221	72.14	0.9784
3	17.69	0.90704	15.19	0.93887	13.23	0.93519	11.55	0.9479	14.415	0.9655
4	87.66	0.93992	73.97	0.96534	70.74	0.96582	64.86	0.97615	74.3075	0.9807
5	18.33	0.91532	14.69	0.94524	13.74	0.94313	12.02	0.95575	14.695	0.9694
6	90.18	0.94477	76.08	0.96909	72.77	0.96963	66.73	0.97949	76.44	0.9827
7	86.01	0.9393	72.56	0.96487	69.39	0.96532	63.62	0.97582	72.895	0.9804
8	74.87	0.91272	63.21	0.94318	60.39	0.94322	55.33	0.95539	63.45	0.9688
9	100.88	0.96148	85.03	0.98131	81.38	0.98205	74.64	0.98991	85.4825	0.9893
10	7.006	0.86434	5.01	0.89136	4.43	0.87439	3.38	0.87448	4.9565	0.9360
11	11.198	0.09045	8.59	0.93497	7.87	0.92978	6.57	0.94226	8.557	0.8007
12	14.58	0.91878	11.48	0.94818	10.64	0.94553	9.14	0.95831	11.46	0.9709
13	19.63	0.9302	15.79	0.95796	14.79	0.9568	12.98	0.96889	15.7975	0.9764
14	28.07	0.93954	22.98	0.96541	21.71	0.96517	19.39	0.97621	23.0375	0.9806
15	32.26	0.94226	26.56	0.96749	25.15	0.96746	22.58	0.97814	26.6375	0.9817
16	44.89	0.94723	37.34	0.97118	35.51	0.9715	32.18	0.98143	37.48	0.9838
17	70.14	0.95164	58.89	0.97433	56.24	0.97489	51.38	0.98412	59.16	0.9855
18	95.395	0.95365	80.44	0.97574	76.97	0.97639	70.58	0.98538	80.8463	0.9863
19	145.903	0.95556	123.55	0.97705	118.42	0.97778	112.09	0.98729	124.991	0.9871
20	196.41	0.95647	166.65	0.97767	159.87	0.97843	147.38	0.98682	167.578	0.9873
21	-	-	-	-	-	-	-	-	-	-
22	5.147	0.73859	3.45	0.73199	2.93	0.67627	2.01	0.58807	3.38425	0.8260
23	8.72	0.82615	6.51	0.85362	5.87	0.83636	4.74	0.83407	6.46	0.9152
24	15.92	0.87881	12.67	0.9117	11.79	0.90679	10.23	0.91877	12.6525	0.9508
25	37.45	0.91186	31.11	0.94242	29.53	0.94172	26.68	0.95421	31.1925	0.9682
26	58.99	0.92013	49.55	0.94941	47.26	0.94939	43.13	0.96134	49.73	0.9721
27	80.53	0.92386	67.98	0.95248	64.99	0.95271	59.57	0.96435	68.2675	0.9738
28	42.92	0.93951	35.69	0.96521	33.93	0.96533	30.73	0.97601	35.8175	0.9805
29	42.28	0.93678	35.15	0.96305	33.41	0.9631	30.26	0.97402	35.275	0.9794
30	42.28	0.93678	35.15	0.96305	33.41	0.96309	30.26	0.97402	35.275	0.9794
31	41.02	0.93104	34.1	0.95844	32.4	0.95832	29.32	0.96969	34.21	0.9769
32	41.02	0.93104	34.1	0.95844	32.4	0.95832	29.32	0.9697	34.21	0.9769
33	31.18	0.86506	25.84	0.90057	24.46	0.89814	22.01	0.91152	25.8725	0.9454
34	25.97	0.80871	21.45	0.84664	20.23	0.84165	18.12	0.85352	21.4425	0.9152
35	21.69	0.74547	17.81	0.7828	16.73	0.77438	14.88	0.7819	17.7775	0.8781
36	10.45	0.88677	7.68	0.812	6.99	0.79932	5.66	0.73135	7.695	0.8980
37	53.53	0.97089	44.56	0.98749	42.46	0.98841	38.56	0.99498	44.7775	0.9927
38	2.42	0.63146	0.96	0.17403	0.53	0.01339	−0.28	−0.0640	0.9075	-
39	-	-	-	-	-	-	-	-	-	-
40	-	-	-	-	-	-	-	-	-	-
41	26.53	0.92462	21.13	0.88736	19.93	0.8856	17.54	0.86171	21.2825	0.94323

-: The result is invalid.

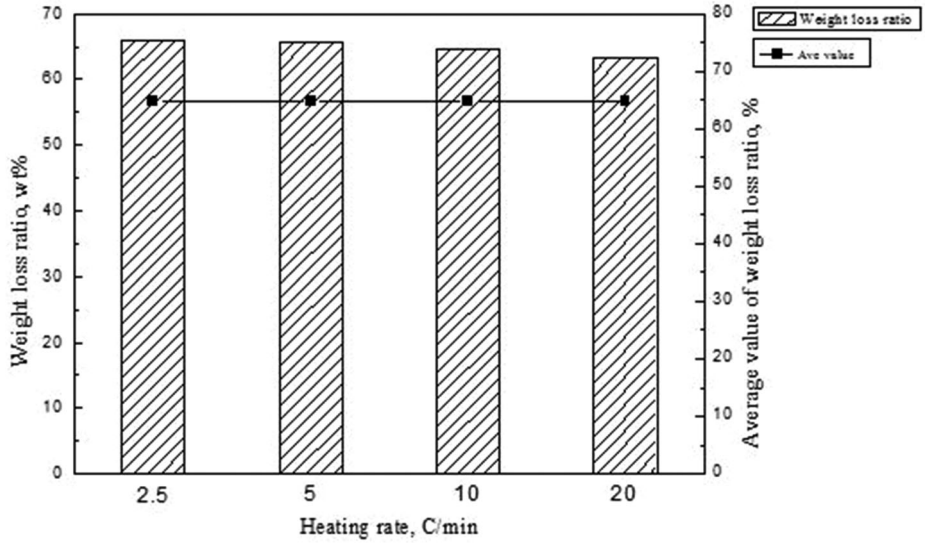

Figure 4. Weight losses of MDEA + PZ solution at different heating rates.

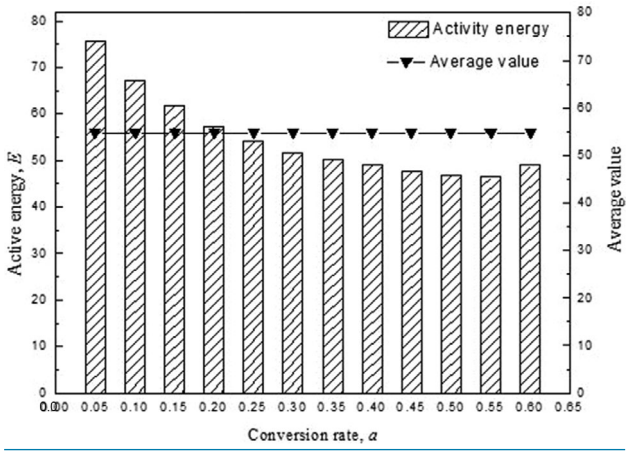

Figure 5. Activity energy E of MDEA + PZ-rich amine solution with FWO method.

energy values of No. 17 and 26 mechanism functions were 59.16 and 49.73 kJ mol^{-1}, respectively, which were apparently both closed to the result of FWO method 54.76 kJ mol^{-1}. However the relative error of No. 17 was 8.04% which was smaller than 9.18% of No. 26. Thus it could preliminary determine the No. 17 as aimed function.

Moreover, as shown in Table 3, the correlation coefficient of No. 17 was 0.9855, which was higher than that of No. 26, 0.9721. The results of linear fitting for No. 17 at four heating rates were shown in Fig. 6. It apparently illustrated that No. 17 mechanism function had a good linear correlation. Therefore, the No. 17 was selected as the most probable mechanism function

Table 4. Kinetic parameters of No. 17 mechanism function for MDEA + PZ solution.

	E (kJ mol^{-1})	A	R
$\beta = 2.5$ °C min^{-1}	70.14	2.17×10^9	0.9755
$\beta = 5$ °C min^{-1}	58.89	3.34×10^7	0.9871
$\beta = 10$ °C min^{-1}	56.24	1.37×10^7	0.9874
$\beta = 20$ °C min^{-1}	51.38	1.95×10^6	0.9920
Ave	59.16	5.54×10^8	0.9855

for CO_2 desorption from MDEA + PZ rich amine aqueous solution.

After confirming the No. 17 as the most probable mechanism function, the kinetic parameters of No. 17 mechanism function under different heating rates were calculated with CR method and the results were shown in Table 4. The average activation energy E was 59.16 kJ mol^{-1}, the preexponential factor A was 5.54×10^8, the most probable integral mechanism function was $G(\alpha) = [-\ln(1-\alpha)]^{3/2}$, the most probable differential mechanism function was $f(\alpha) = 2/3(1-\alpha)(-\ln(1-\alpha))^{-1/2}$, and reaction constant acquired according with Arrhenius equation was as following:

$$k = 5.54 \times 10^8 exp\left(\frac{-7115}{T}\right) \quad (6)$$

Comparison of kinetic parameters for three rich amine aqueous solutions

The kinetic parameters of three rich amine aqueous solutions (MDEA, MDEA + DEA, and MDEA + PZ)

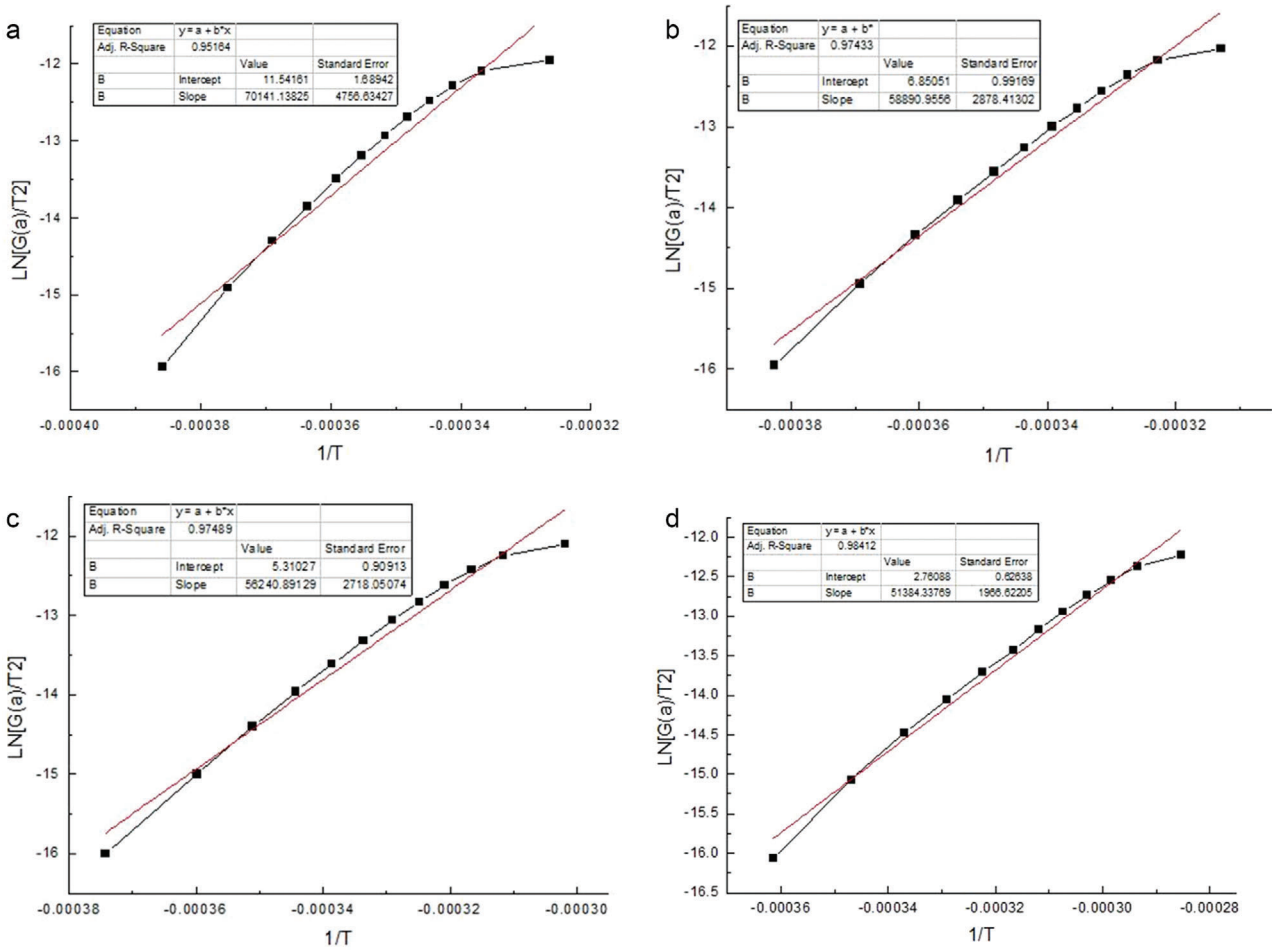

Figure 6. Linear fitting results of No. 17 mechanism function by CR method: (a) 2.5 °C min^{-1}, (b) 5 °C min^{-1}, (c) 10 °C min^{-1}, and (d) 20 °C min^{-1}.

Table 5. The kinetic parameters for three rich amine solutions.

Rich amine solution	Activation energy E, kJ mol^{-1}	Preexponential factor A	Mechanism functions $G(\alpha)$	Differential mechanism function $f(\alpha)$
MDEA	50.36	1.68×10^7	$\alpha^{3/2}$	$2/3\alpha^{-1/2}$
MDEA + DEA	59.68	2.22×10^7	$[(1+\alpha)^{1/3}-1]^2$	$3/2(1+\alpha)^{2/3}((1+\alpha)^{1/3}-1)^{-1}$
MDEA + PZ	59.16	5.54×10^8	$[-\ln(1-\alpha)]^{3/2}$	$2/3(1-\alpha)(-\ln(1-\alpha))^{-1/2}$

were concluded in Table 5. The effects of activator on desorption characteristics were discussed by comparing kinetic parameters.

Activation energy

The desorption rate constant is closely related to activation energy on the basis of Arrhenius equation. In generally, larger activation energy for desorption means that the rich amine aqueous solution needs more energy for desorption and it is harder to be desorbed. It could be seen in Table 5 that the average activation energy values for three rich amine aqueous solutions were respectively 50.36, 59.68, and 59.16 kJ mol^{-1}. The order of activation energy for three rich amine aqueous solution was $E_{MDEA} < E_{MDEA+PZ} < E_{MDEA+DEA}$. It was inferred that the order of desorption rate was MDEA > MDEA + PZ > MDEA + DEA on the respect of activation energy.

Thus the activator PZ and DEA could increase absorption rate of MDEA and benefited for the

absorption process but the desorption rate would be decreased. Although absorption rate is an important factor on choosing adsorbent, it should consider both absorption and desorption rate comprehensively for selecting a proper adsorbent.

Preexponential factor

The preexponential factor can be explained as the number of effectively colliding molecules by the 'collision theory'. Larger preexponential factor means that it has more opportunities for absorbents colliding and reacting with CO_2. Since the order was $A_{MDEA} < A_{MDEA+DEA} < A_{MDEA+PZ}$ in Table 5, it was indicated that the absorption rate of MDEA + PZ was larger than MDEA and MDEA + DEA, and the desorption rate of MDEA was larger than MDEA + DEA and MDEA + PZ. Thus on the perspective of preexponential factor, the order of desorption rate was MDEA>MDEA + DEA>MDEA + PZ.

Kinetic model

The mechanisms functions of CO_2 desorption from three rich amine aqueous solutions were determined according to the thermal analysis kinetic method. The desorption rate constants k_1, k_2, and k_3 for three rich amine aqueous solutions at different heating rates were calculated with Eqn (7).

$$k = Ae^{-E/RT} \tag{7}$$

The desorption rate kinetic equation was as follows:

$$\frac{d\alpha}{dt} = kf(\alpha) \tag{8}$$

Take kinetic parameters in Table 5 into Eqns (7) and (8), and desorption kinetic equation could be calculated as Eqn (9):

$$\frac{d\alpha}{dt} = A \cdot exp\left(\frac{E}{RT}\right) \cdot f(\alpha) \tag{9}$$

For MDEA rich amine aqueous solution,

$$\frac{d\alpha}{dt} = 1.12 \times 10^7 \alpha^{-1/2} exp\left(\frac{-6057}{T}\right) \tag{10}$$

For MDEA–DEA rich amine aqueous solution,

$$\frac{d\alpha}{dt} = 3.33 \times 10^7 (1+\alpha)^{2/3} [-ln\,(1-\alpha)]^{-1} \times exp\left(\frac{-7178}{T}\right) \tag{11}$$

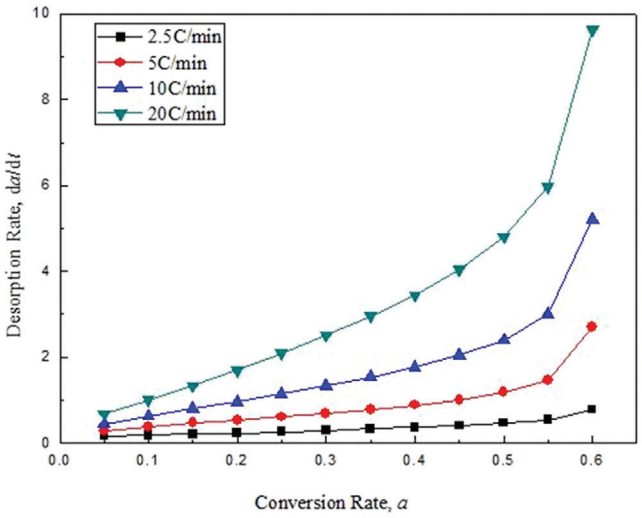

Figure 7. Desorption rate for MDEA-rich amine solution.

For MDEA–PZ rich amine aqueous solution,

$$\frac{d\alpha}{dt} = 3.69 \times 10^8 (1-\alpha) [-ln\,(1-\alpha)]^{-1/2} \times exp\left(\frac{-7115}{T}\right) \tag{12}$$

As shown in Table 6, the average desorption rate of these three rich amine aqueous solutions at different heating rates were 1.597,1.507, and 1.422 s^{-1}, respectively. It was shown that the order of desorption rate was MDEA>MDEA + DEA>MDEA + PZ, which was basically consistent with the results mentioned above with the respects of activation energy and preexponential factor. According with Eqn (9), the desorption kinetic equation is directly affected by activation energy, temperature, preexponential factor and mechanism function. The desorption rate curves for three rich amine aqueous solutions were shown in Figs. 7–9. It was interesting to found that the trends of desorption rates for the three rich amine aqueous solutions were almost the same at hour heating rates. The desorption rates raised with both conversion rate α and heating rate β increasing. The desorption rate of the three amine rich aqueous solutions increased slightly at 2.5 °C min^{-1} and 5 °C min^{-1}, while the desorption rate increased more sharply at 10 °C min^{-1} and 20 °C min^{-1}. It proved that desorption rate could be promoted by increasing heating rate. In addition, it also could observe in Figs. 7–9 that the slopes of desorption rate curves at range of conversion rate 0.55–0.60 were larger than the range of 0–0.55. The

Table 6. Reaction rate of CO_2 desorption for three rich amine solutions at different heating rates.

	$(d\alpha/dt)_{MDEA}$, s^{-1}				$(d\alpha/dt)_{MDEA+DEA}$, s^{-1}				$(d\alpha/dt)_{MDEA+PZ}$, s^{-1}			
B, °C min^{-1}												
A	2.5	5	10	20	2.5	5	10	20	2.5	5	10	20
0.05	0.157	0.275	0.444	0.673	0.205	0.217	0.446	0.643	0.189	0.229	0.377	0.799
0.1	0.178	0.380	0.637	1.004	0.193	0.239	0.536	0.848	0.225	0.334	0.581	1.247
0.15	0.206	0.462	0.803	1.329	0.202	0.288	0.647	1.107	0.258	0.424	0.743	1.705
0.2	0.235	0.536	0.965	1.697	0.219	0.334	0.778	1.446	0.285	0.505	0.891	2.201
0.25	0.265	0.613	1.147	2.082	0.240	0.385	0.926	1.810	0.306	0.580	1.033	2.682
0.3	0.296	0.693	1.339	2.507	0.263	0.443	1.093	2.242	0.323	0.644	1.161	3.163
0.35	0.330	0.783	1.542	2.957	0.293	0.510	1.281	2.728	0.338	0.701	1.282	3.553
0.4	0.368	0.886	1.770	3.444	0.328	0.591	1.505	3.254	0.351	0.749	1.397	3.914
0.45	0.411	1.008	2.039	4.046	0.373	0.691	1.785	3.969	0.364	0.796	1.503	4.342
0.5	0.465	1.174	2.402	4.805	0.438	0.830	2.181	4.861	0.380	0.852	1.630	4.772
0.55	0.547	1.460	2.999	5.976	0.554	1.076	2.861	6.316	0.415	0.945	1.834	5.336
0.6	0.788	2.695	5.202	9.632	1.132	2.185	5.724	11.115	0.637	1.403	2.699	7.179
Ave	0.354	0.914	1.774	3.346	0.370	0.649	1.647	3.362	0.339	0.680	1.261	3.408
	1.597				1.507				1.422			

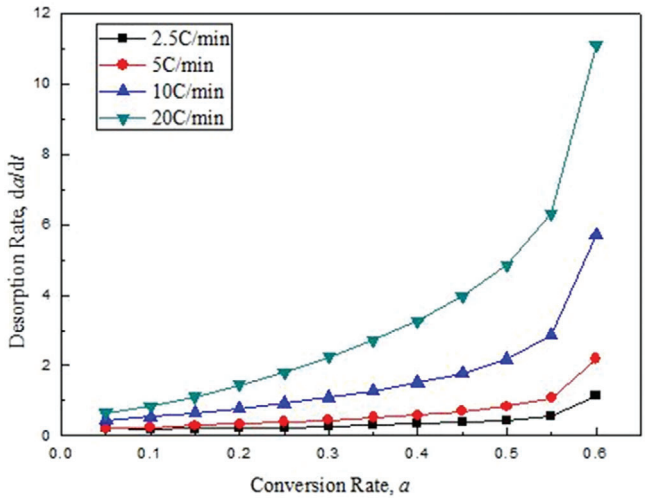

Figure 8. Desorption rate for MDEA + DEA rich amine solution.

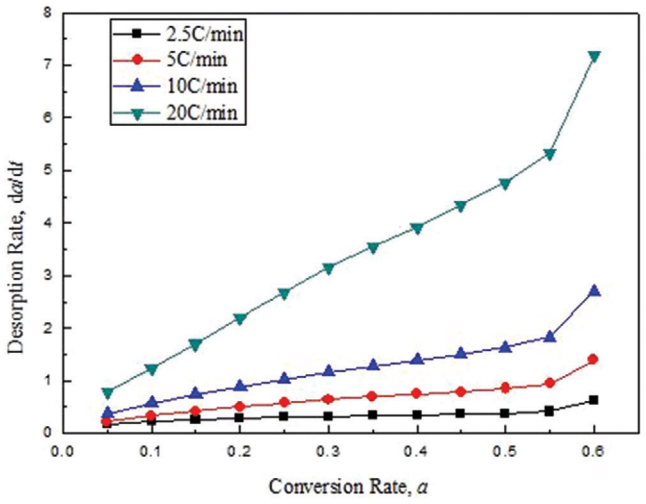

Figure 9. Desorption rate for MDEA – PZ rich amine solution.

increasing of desorption rate was mainly resulted from the heating up of amine aqueous solution, which brought out the break chemical bond between CO_2 and alkanolamine at temperature range of 85–120 °C in Fig. 2.

Since energy penalty was greatly influenced by regeneration, desorption performance should be considered for screening efficient absorbent. High desorption rate means it need low energy requirement for regeneration. It is also well known that absorbents should be selected according to the mechanism of both absorption and desorption. The reaction mechanisms were affected with the structure of different absorbents. The reaction mechanism of absorption and desorption for the three amine aqueous solutions was summarized in Table 7. The results discussed above could also be explained by the mechanisms of absorption and desorption. MDEA can react with CO_2 directly and the

Table 7. Mechanism of absorption and desorption for the three amine solutions.

Solution	Absorption	Desorption
MDEA	$CO_2 + H_2O \Leftrightarrow H^+ + HCO_3^-$ $H^+ + R_1R_2R_3N \Leftrightarrow R_1R_2R_3NH^+$ $CO_2 + R_1R_2R_3N + H_2O \Leftrightarrow R_1R_2R_3NH^+ + HCO_3^-$	$HCO_3^- + H^+ \Leftrightarrow CO_2 + H_2O$ $R_1R_2R_3NH^+ + HO^- \Leftrightarrow R_1R_2R_3N + H_2O$
MDEA + DEA	$R_1R_2NH + CO_2 \Leftrightarrow R_1R_2NH^+COO^-$ $R_1R_2NH^+COO^- + R_1R_2NH \Leftrightarrow R_1R_2NCOO^- + R_1R_2NH_2^+$ $R_1R_2NH^+COO^- + R_1R_2R_3N \Leftrightarrow R_1R_2NCOO^- + R_1R_2R_3NH^+$ $CO_2 + R_1R_2R_3N + H_2O \Leftrightarrow R_1R_2R_3NH^+ + HCO_3^-$	$R_1R_2NCOO^- + H_2O \Leftrightarrow R_1R_2NH + CO_2 + OH^-$ $R_1R_2NH_2^+ + OH^- \Leftrightarrow R_1R_2NH + H_2O$ $R_1R_2R_3NH^+ + OH^- \Leftrightarrow R_1R_2R_3N + H_2O$ $HCO_3^- + H^+ \Leftrightarrow H_2O + CO_2$
MDEA + PZ	$R_1(NH)_2 + 2CO_2 \Leftrightarrow R_1(NHCOO)_2$ $R_1(NHCOO)_2 + 2H_2O \Leftrightarrow R_1(NH_2^+)_2 + 2HCO_3^-$ $R_1(NHCOO)_2 + 2R_1R_2R_3N \Leftrightarrow R_1(NH)_2 + 2R_1R_2R_3NCOO$ $R_1R_2R_3NCOO + H_2O \Leftrightarrow R_1R_2R_3NH^+ + HCO_3^-$	$R_1(NH_2^+)_2 + 2OH^- \Leftrightarrow R_1(NH_2) + 2H_2O$ $R_1R_2R_3NH^+ + OH^- \Leftrightarrow R_1R_2R_3N + H_2O$ $HCO_3^- + H^+ \Leftrightarrow H_2O + CO_2$

absorption reaction consists of two steps. The CO_2 molecules dissolve into the liquid firstly, and then CO_2 reacts with MDEA to form bicarbonate.[11,31] As there is no hydrogen atom connected with MDEA and then the chemical activity is not as good as primary amine or secondary amine. The primary and secondary amines (MEA and DEA) with active hydrogen atoms can form zwitterion ion with CO_2 quickly, and the zwitterion ion are transferred to the liquid bulk to react with MDEA to form stable carbamate sequentially.[11,22] The absorption mechanism of PZ and CO_2 is similar with DEA. PZ can quickly combine with CO_2 and form carbamate, which is transferred to the liquid phase MDEA. At the same time, carbamate reacts with MDEA to form bicarbonate, and PZ is recycled. Thus, PZ is regarded as a 'catalyst' for the absorption process.[32]

The desorption is reversed with absorption. The metastable bicarbonate formed during absorption process is easy to regenerate, so the desorption rate of MDEA is the highest. Nevertheless carbamate with better stability decomposed slower than bicarbonate, so the desorption rate of MDEA + DEA is slower than MDEA rich amine aqueous solution. The result was consistent with literature[33] that tertiary amine had greater regeneration behaviors but worse CO_2 absorption rates than primary and secondary amines. In addition PZ with two symmetric nitrogen atoms can combine with CO_2 firmly and adsorb CO_2 promptly. The carbamate formed by CO_2 and PZ is more stable. Furthermore 1 mol PZ can react with 2 mol CO_2. It resulted in the low reaction rate and more energy of desorption. So the desorption rate of MDEA + PZ was the slowest. It is commonly recognized that the desorption rate is affected by experimental equipment, operation condition, mass transfer models, and physical data such as species diffusivity and CO_2 solubility, and so on. Since there are significant differences between TG analyzer and experimental equipment, the results absolute value of TG method may not the same with common experimental equipment. The TGA method was suit for preliminary screening absorbent without building apparatus in experiment.

Conclusions

In order to select appropriate absorbents with excellent potential of desorption performance in experiment, the CO_2 desorption process of 3.25 mol L^{-1} MDEA + 0.1mol L^{-1} PZ rich amine aqueous solutions was studied with TGA method. The desorption process of MDEA + PZ rich amine aqueous solutions could be divided into two stages. The CO_2 and H_2O were desorbed from rich amine aqueous solution at temperature range of 85–120 °C in the first stage and the MDEA and PZ with higher boiling points evaporated in the second stage. The TGA results of MDEA, MDEA + DEA, and MDEA + PZ rich amine aqueous solutions were consistent well.

The CO_2 desorption kinetic parameters (activation energy, the preexponential factor, and the most probable mechanism function) of MDEA + PZ rich amine aqueous solution were determined via thermal analysis kinetic, FWO, and CR methods. The kinetic parameters for three rich amine aqueous solutions (MDEA, MDEA + DEA, and MDEA + PZ) were comprehensively compared and desorption rate models were established. The order of desorption rate predict by kinetic models was MDEA>MDEA + DEA>MDEA + PZ. It proved that the TGA method

was an effective method to study CO_2 desorption kinetics quickly in laboratory without setting up complex desorption tower, and provide theoretical basis for absorbent selection, although there is error between TGA instrument and stripper apparatus. It will quickly provide preliminary basis for adsorbents by the comparison of desorption performance for different amine aqueous solutions in laboratory with TGA and thermal analysis kinetics methods. It also would be applied for other amine aqueous solutions.

Conflict of Interest

We declare that we have no financial and personal relationships with other people or organizations that can inappropriately influence our work, there is no professional or other personal interest of any nature or kind in any product, service, and/or company that could be construed as influencing the position presented in, or the review of the manuscript entitled.

References

1. Wu Z, Li W, Zhu T, Zheng Y, Wang T, Wang C *et al*., Investigation of CO_2 absorption kinetics and desorption performance in aqueous 1–(2–aminoethyl)–3–methylimidazolium bromine solution. *Energy Fuel* **32**:6934–6942 (2018).
2. Bauer A and Menrad K, Standing up for the Paris Agreement: Do global climate targets influence individuals' greenhouse gas emissions? *Environ Sci Policy* **99**:72–79 (2019).
3. Li W, Xiao S, Liu S, Liu H and Liang Z, Comparative kinetics of homogeneous reaction of CO_2 and unloaded/loaded amine using stopped–flow technique: A case study of MDEA solution. *Sep Pur Tech* **242**:116833 (2020).
4. Ayittey FK, Obek CA, Saptoro A, Perumal K and Wong MK, Process modifications for hot potassium carbonate-based CO_2 capture system: A comparative study. *GREENH GASES* **0**:1–17 (2020).
5. Nozaeim AA, Tavasoli A, Mortaheb HR and Mafi M, CO_2 absorption/desorption in aqueous DEEA/MDEA and their hybrid solutions with sulfolane. *J Nat Gas Sci Eng* **76**:1–11 (2020).
6. Li L, Liu Y, Wu K, Liu C, Tang S and Yue H, Catalytic solvent regeneration of a CO_2 –loaded MEA solution using an acidic catalyst from industrial rough metatitanic acid. *Greenh Gases* **0**:1–12 (2018).
7. Sahoo PC, Kumar M, Singh A, Singh MP, Puri SK and Ramakumar SSV, Accelerated CO_2, capture in hybrid solvent using co–immobilized enzyme/complex on a hetero–functionalized support. *J CO2 Utilization* **21**:77–81 (2017).
8. Sema T, Naami A, Fu K, Edali M, Liu H and Shi H, Comprehensive mass transfer and reaction kinetics studies of CO_2 absorption into aqueous solutions of blended MDEA–MEA. *Chem Eng J* **209**:501–512 (2012).
9. Khan AA, Halder G and Saha AK, Experimental investigation on efficient carbon dioxide capture using piperazine (PZ) activated aqueous methyldiethanolamine (MDEA) solution in a packed column. *Int J Greenhouse Gas Control* **64**:163–173 (2017).
10. Li N, Du SJ, Zhang SN, Zhang K and Wu WF, Desorption kinetic of CO_2 in mixed amine of MDEA–TETA. *Chem Eng* **45**:65–68 (2017).
11. Zhang T, Yu Y and Zhang Z, An interactive chemical enhancement of CO_2 capture in the MEA/PZ/AMP/DEA binary solutions. *Int J Greenhouse Gas Control* **74**:119–129 (2018).
12. Luo Q, Feng B, Liu Z, Zhou Q, Zhang Y and Li N, Experimental study on simultaneous absorption and desorption of CO_2, SO_2, and NOx using aqueous N–Methyldiethanolamine and dimethyl sulfoxide solutions. *Energy Fuel* **32**:3647–3659 (2018).
13. Puxty G and Rowland R, Modeling CO_2 mass transfer in amine mixtures: PZ–AMP and PZ–MDEA. *Environ Sci Technol* **45**:2398–2405 (2011).
14. Khan AA, Halder G and Saha AK, Kinetic effect and absorption performance of piperazine activator into aqueous solutions of 2–amino–2–methyl–1–propanol through post–combustion CO_2 capture. *Korean J Chem Eng* **36**:1090–1101 (2019)
15. Xu G, Zhang C, Qin S and Wang Y, Kinetics study on absorption of carbon dioxide into solutions of activated methyldiethanolamine. *Ind Eng Chem Res* **31**:921–927 (1992).
16. Ali BS and Aroua MK, Effect of piperazine on CO_2 loading in aqueous solutions of MDEA at low pressure. *Int J Thermophys* **25**:1863–1870 (2014).
17. Ying J, Raets S and Eimer D, The activator mechanism of piperazine in aqueous methyldiethanolamine solutions. *Energy Procedia* **114**:2078–2087 (2017).
18. Xu GW, Zhang CF, Qin SJ and Zhu B-C, Desorption of CO_2 from MDEA and activated MDEA solutions. *Ind Eng Chem Res* **34**:874–880 (1995).
19. Cadours R, Bouallou C, Gaunand A and Richon D, Kinetics of CO_2 desorption from highly concentrated and CO_2–loaded methyldiethanolamine aqueous solutions in the range 312–383K. *Ind Eng Chem Res* **36**:20 (1997) .
20. Jamal A, Meisen A and Lim C, Kinetics of carbon dioxide absorption and desorption in aqueous alkanolamine solutions using a novel hemispherical contactor–I. Experimental apparatus and mathematical modeling. *Chem Eng Sci* **61**:6571–6589 (2006).
21. Wang T, He H, Yu W, Sharif Z and Fang M, Process simulations of CO_2 desorption in the interaction between novel direct steam stripping process and solvents. *Energy Fuel* **31**:4255–4262 (2017).
22. Zhang R, Zhang X, Yang Q, Yu H, Liang Z and Luo X, Analysis of the reduction of energy cost by using MEA–MDEA–PZ solvent for post–combustion carbon dioxide capture (PCC). *Appl Energy* **205**:1002–1011 (2017).
23. Aghel B, Sahraei S and Heidaryan E. Carbon dioxide desorption from aqueous solutions of monoethanolamine and diethanolamine in a microchannel reactor. *Sep Pur Tech* **237**:116390 (2019).
24. Barzagli F, Mani F and Peruzzini M, A 13C NMR investigation of CO_2 absorption and desorption in aqueous 2,2′–iminodiethanol and N–methyl–2,2′–iminodiethanol. *Int J Greenhouse Gas Control* **5**:448–456 (2011).
25. Listiyana NI, Rahmawati Y, Nurkhamidah S, Syahmur HR and Zaelane Y, CO_2 desorption from activated DEA using

membrane contactor with vacuum regeneration technology. *MATEC Web Conferences* **156**:1–6 (2018).
26. Liu H, Zhao S, Zhou F, Yao C and Chen G, Ultrasonic enhancement of CO_2 desorption from MDEA solution in microchannels. *Ind Eng Chem Res* **58**:1711–1719 (2019).
27. Kang S, Shen X and Yang W, Investigation of CO_2 desorption kinetics in MDEA and MDEA+DEA rich amine solutions with thermo–gravimetric analysis method. *Int J Greenhouse Gas Control* **95**:1–8 (2020).
28. Shen X, Xiao Y, Xu L, Xuan A and Wu Y, Determination of CO_2 solubility in N–methyldiethanolamine aqueous solution for combination of medium temperature shift with pressure swing adsorption. *Petrochem Technol* **39**:280–284 (2010).
29. Hu R, *Pyrolysis and Kinetic Analysis*. Science Press, Beijing, China (2008).
30. Jayaraman K, Kk MV and Gkalp I, Combustion mechanism and model free kinetics of different origin coal samples: Thermal analysis approach. *Energy* **204**:1–9 (2020).
31. Liu H, Hong R, Xiang C, Wang H, Li Y, Xu G *et al*., Thermal decomposition kinetics analysis of the oil sludge using model–based method and model–free method. *Process Saf Environ* **141**:167–177 (2020).
32. Saidi M, Rate–based modeling of CO_2 absorption into piperazine–activated aqueous N–methyldiethanolamine solution: kinetic and mass transfer analysis. *Int J Chem Kinet* **49**:690–708 (2017).
33. Wang Z, Fang MX and Pan YL, Amine–based absorbents selection for CO_2 membrane vacuum regeneration technology by combined absorption–desorption analysis. *Chem Eng Sci* **93**:238–249 (2013).

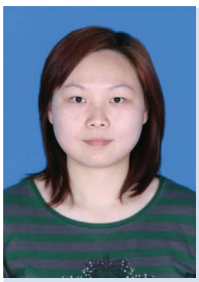

Shunji Kang

Shunji Kang is a doctoral candidate at Wuhan Institute of Technology. Her research focuses on petroleum chemical engineering, chemical separation technology and environmental engineering.

Zhi Shen

Zhi Shen is graduated in the field of chemical engineering Wuhan Institute of Technology. His research focuses on petroleum refining engineering, especially desulfurization of fuel and the biomedical organic polymer material.

Xizhou Shen

Xizhou Shen holds a position of at school of Chemical Engineering and Pharmacy, Wuhan Institute of Technology. Professor Shen has over 25-year research and engineering experience in the field of petroleum refining and he has received the National Invention Award, provincial and municipal scientific and technological progress award.

Liuya Fang

Liuya Fang is a doctoral candidate at Wuhan Institute of Technology. His research focuses on petroleum and natural gas industry, carboncapture, utilization, and storage.

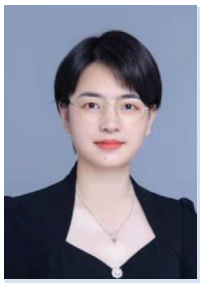

Li Xiang

Li Xiang is a teacher at the College of Post and Telecommunication of WIT. His research focuses on heavy oil processing, road asphalt technology development and chemical separation technology.

Wenze Yang

Wenze Yang is an engineer work at Central Southern China Electric Power Design Institute in Wuhan. She is mainly engaged in pipeline design of chemical process.